Identification and validation of novel microenvironment-based immune molecular subgroups of head and neck squamous cell carcinoma : implications for immunotherapy

Reference:
Chen Y. -P., Wang Y. -Q., Lv J. -W., Li Y. -Q., Chua M. L. K., Le Q. -T., Lee N., Colevas A. Dimitrios, Seiwert T., Hayes D. N., ...- Identification and validation of novel microenvironment-based immune molecular subgroups of head and neck squamous cell carcinoma : implications for immunotherapy
Annals of oncology / European Society for Medical Oncology - ISSN 0923-7534 - 30:1(2019), p. 68-75
Full text (Publisher's DOI): https://doi.org/10.1093/ANNONC/MDY470

Title page

Identification and validation of novel microenvironment-based immune molecular subgroups of head and neck squamous cell carcinoma: implications for immunotherapy

Running title: Virtual Microdissection Reveals HNSC Immune Molecular Subgroups

Authors list:

Y.-P. Chen, [1]* Y.-Q. Wang, [1]* J.-W. Lv, [1]* Y.-Q. Li, [1]* M. L. K. Chua, [2] Q.-T. Le, [3] N. Lee, [4.] A. Dimitrios Colevas, [5] T. Seiwert, [6] D. N. Hayes, [7] N. Riaz, [4] J. B. Vermorken, [8] B. O'Sullivan, [9] Q.-M. He, [1] X.-J. Yang, [1] L.-L. Tang, [1] Y.-P. Mao, [1,10] Y. Sun, [1] N. Liu, [1,11]† J. Ma, [1]†

Affiliations list:

1. Department of Radiation Oncology, Sun Yat-sen University Cancer Center, State Key Laboratory of Oncology in South China, Collaborative Innovation Center for Cancer Medicine, Guangdong Key Laboratory of Nasopharyngeal Carcinoma Diagnosis and Therapy, Guangzhou, People's Republic of China

2. Division of Radiation Oncology, National Cancer Centre Singapore; Oncology Academic Clinical Programme, Duke-NUS Medical School, Singapore

3. Department of Radiation Oncology, Stanford University, Stanford, CA, USA

4. Department of Radiation Oncology, Memorial Sloan Kettering Cancer Center, New York, NY, USA

5. Department of Medicine, Division of Oncology, Stanford University, Stanford, CA, USA

6. Department of Medicine, The University of Chicago, Chicago, IL, USA.

7. Lineberger Comprehensive Cancer Center, University of North Carolina at Chapel Hill, Chapel Hill, North Carolina, USA

8. Department of Medical Oncology, Antwerp University Hospital, Edegem, Belgium

9. Ontario Cancer Institute, University Health Network, Toronto, Ontario, Canada

10. Department of Radiation Oncology, University of Michigan, Ann Arbor, MI, USA

11. Department of Experimental Radiation Oncology, The University of Texas MD Anderson Cancer Center, Houston, TX, USA

* These authors contributed equally to this work.

†**Corresponding authors**:

Jun Ma, Department of Radiation Oncology, Sun Yat-sen University Cancer Center, State Key Laboratory of Oncology in South China, Collaborative Innovation Center for Cancer Medicine, Guangdong Key Laboratory of Nasopharyngeal Carcinoma Diagnosis and Therapy, 651 Dongfeng Road East, Guangzhou 510060, People's Republic of China.

Tel.:+86-20-87343469; **Fax:**+86-20-87343295

E-mail: majun2@mail. sysu.edu.cn

Na Liu, Department of Radiation Oncology, Sun Yat-sen University Cancer Center, State Key Laboratory of Oncology in South China, Collaborative Innovation Center for Cancer Medicine, Guangdong Key Laboratory of Nasopharyngeal Carcinoma Diagnosis and Therapy, 651 Dongfeng Road East, Guangzhou 510060, People's Republic of China;

Department of Experimental Radiation Oncology, The University of Texas MD Anderson Cancer Center, Houston, TX, USA

Tel.:+86-20-87343469; **Fax:**+86-20-87343295; **E-mail:** liun1@sysucc.org.cn

ABSTRACT

***Background*:** Targeting the immune checkpoint pathway has demonstrated anti-tumor cytotoxicity in treatment-refractory head and neck squamous cell carcinoma (HNSC). To understand the molecular mechanisms underpinning its anti-tumor response, we characterized the immune landscape of HNSC by their tumor and stromal compartments to identify novel immune molecular subgroups.

Patients and methods: A training cohort of 522 HNSC samples from the Cancer Genome Atlas profiled by RNA sequencing was analyzed. We separated gene expression patterns from tumor, stromal, and immune cell gene using a non-negative matrix factorization algorithm. We correlated the expression patterns with a set of immune-related gene signatures, potential immune biomarkers, and clinicopathological features. Six independent datasets containing 838 HNSC samples were used for validation.

Results: Approximately 40% of HNSCs in the cohort (211/522) were identified to show enriched inflammatory response, enhanced cytolytic activity and active interferon-γ signaling (all, $P < 0.001$). We named this new molecular class of tumors the Immune Class. Then we found it contained two distinct microenvironment-based subtypes, characterized by markers of active or exhausted immune response. The Exhausted Immune Class was characterized by enrichment of activated stroma and anti-inflammatory M2 macrophage signatures, WNT/TGF-β signaling pathway activation and poor survival (all, $P < 0.05$). An enriched proinflammatory M1 macrophage signature, enhanced cytolytic activity, abundant tumor-infiltrating lymphocytes (TILs), high human papillomavirus (HPV) infection and favorable prognosis was associated with Active Immune Class (all, $P < 0.05$). The robustness of these immune molecular subgroups was verified in the validation cohorts,

and Active Immune Class showed potential response to PD-1 blockade ($P = 0.01$).

Conclusions: This study revealed a novel Immune Class in HNSC; two subclasses characterized by active or exhausted immune responses were also identified. These findings provide new insights into tailoring immunotherapeutic strategies for different HNSC subgroups.

Keywords: head and neck squamous cell carcinoma, tumor-immune microenvironment, immune molecular subgroups, virtual microdissection, immune checkpoint blockade

Key Message: In this multiple-cohort study analyzing gene expression profiles of 1,360 HNSC samples, we identified molecular subgroups (Active, Exhausted & non-Immune) with different immunobiological traits using virtual microdissection. The novel immune molecular subgroups prognosticate patients and predict immunotherapy response, aiding in immunotherapy decision-making for different HNSC patient subgroups.

INTRODUCTION

Promising responses have been reported recently with anti-PD-1 therapy in advanced head and neck squamous cell carcinoma (HNSC) [1-4]. However, these agents benefit only a subset of patients [5]. Identifying potential therapeutic markers associated with treatment response or resistance would allow tailoring of appropriate immunotherapy for different patient subgroups. Still, unfortunately, little is known about the HNSC tumor immune milieu and how this information can be leveraged to tailor appropriate immunotherapy for different patient subgroups.

The tumor microenvironment of HNSC is comprised of stromal cellular elements that are admixed with immune cells, particularly at the tumour-stromal interphase [6]. Non-negative matrix factorization (NMF) is an approach established to dissect the molecular signals deriving from these distinct compartments virtually, aiding the evaluation of the complexities of tumor–immune interactions [7, 8]. Using a NMF algorithm, we aimed to isolate immune-related genomic signals from bulk gene expression data in HNSC tumors, and characterized various immune landscapes in this study.

METHODS

We analyzed the gene expression profiles from a total of 1,360 HNSC human samples (**Fig. S1**). A training cohort of 522 samples from The Cancer Genome Atlas (TCGA), profiled by RNA sequencing was included (**Table S1**). Six publicly available datasets profiled by microarray that included 838 HNSC samples were used for further validation (**Table S1**). Tumor, stromal, and immune cell transcriptome profiling data in the training TCGA set were microdissected virtually using unsupervised NMF as previously described [7, 9]. Immune-related gene signatures (**Table S2**) representing different immune statuses or

immune cells were used to characterize immune molecular subgroups using single-sample gene set enrichment analysis (ssGSEA) and Nearest Template Prediction (NTP). For detailed descriptions of all methods, see the **Supplementary Materials**.

RESULTS

Identification of a novel HNSC Immune Class

We first performed NMF of 522 samples in the training cohort from The Cancer Genome Atlas (TCGA) (**Fig. S1**) to extract gene expression signatures related to immune pathways. We confirmed that one of the NMF-identified clusters was linked to inflammatory markers and immune cells, which has been corroborated by an observed high immune enrichment score as previously reported [8, 10] (**Fig. S2A)**. Therefore, this expression pattern was defined as an NMF immune factor. Analysis of the exemplar genes that defined the immune factor confirmed immune-related functions and signaling (**Fig. S2B**). Consensus clustering of exemplar genes and random forest refinement (**Fig. S3A)** identified a new molecular immune phenotype present in 40% of the cohort (211/522), which we refer herein as "Immune Class" (**Fig. S3B**). Patients with Immune Class showed significant enrichment of signatures identifying immune cells (e.g., immune cell subsets, T cells, B cells, macrophages), immune metagenes (e.g., T.NK. and B.P. metagenes), and enhanced cytolytic activity (all, P <0.001) (**Fig. 1A**); among the signatures, we also observed enrichment of the 6-gene interferon (IFN) signature that was previously reported to predict for pembrolizumab response in HNSC (P <0.001) [11]. Class comparison identified 115 genes that were significantly overexpressed in Immune versus non-Immune Classes (**Table S3**). These sets of genes were further defined an immune classifier that included immune-

related genes such as T cell costimulatory molecules (*CD40LG*), B cell surface molecules (*CD19*), IFN-γ (*IFNG*), and chemoattractants (*CCL1*, *CCL25*). Similarly, GSEA identified immune cell signaling enrichment, immune response signaling, and IFN-related signaling (all, FDR <0.05, **Fig. S4, Table S4**).

Immune Class is highlighted by two distinct microenvironmental conditions

Given that immune system exerts both anti- and pro-tumor activity, we next sought to explore the type of immune modulation occurring in response to the tumor microenvironment within the Immune Class. **Fig. 1B** shows that 27% of Immune Class (56/211) was characterized by the previously reported activated stromal gene signature that captures the activated inflammatory stromal response [7]. Patients with the activated stromal gene signature were associated with higher stromal enrichment score and macrophage signatures, and low expression of B cell cluster, B/P metagene signatures and cytolytic activity (all, P <0.05). Besides, the presence of activated stroma was significantly associated with M2 (anti-inflammatory) macrophages and other immunosuppressive components, e.g., the WNT/TGF-ß signaling signature (all, P <0.001). Conversely, in patients lacking the activated stroma signature, we observed high expression of the proinflammatory M1 macrophage signature (P <0.001), although signatures relating to the immune enrichment score and IFN signaling did not differ between the subgroups. We therefore coined these two clusters Exhausted and Active Immune Classes respectively. Analysis of class comparison was shown in **Table S5**. GSEA confirmed the driver role of the WNT/TGF-β signaling pathways, as well as enrichment of epithelial-mesenchymal transition-, angiogenesis-, and metastasis-related pathways in the Exhausted subtype

(**Table S6**).

We next sought to integrate these immune molecular subgroups with the four HNSC molecular classes. We detected a significantly lower proportion of Immune Class within the basal and classical subtypes compared to the mesenchymal and atypical subtypes (18% and 10% vs. 58% and 63%, P <0.001; **Fig. S5A**). We also observed a higher frequency of Active Immune Class in the atypical molecular subtypes (61%), while the mesenchymal type of tumors harbored a higher proportion of the Exhausted Immune Class (42%) (P <0.001). For the integration with the six pan-cancer immune subtypes, we found that about 99% of HNSC patients belong to the wound healing (25%) or IFN-γ dominant (74%) subtypes, while other subtypes only account for 1% of HNSC samples (**Fig. S5B**). The pan-cancer IFN-γ dominant subtype may benefit from immunotherapy, and as expected, a significant higher proportion of Active Immune Class (35%) were shown in this subtype.

Immune Class tumors were associated with tumor-infiltrating lymphocytes (TIL) enrichment and lower copy number alteration burden

Next, we performed immunophenotyping to gain further biological insight into the immunological nature of the Immune Class. Significantly higher rates of moderate (33% vs. 19%) and high (41% vs. 13%) TIL scores were observed in the Immune Class versus the non-Immune class tumors (P =0.01) (**Fig. S6**). Interestingly, patients with Immune Class had relatively lower driver gene gain (P =0.001) and loss (P =0.004) burdens (**Fig. S7A, B**). However, immune molecular subgroups did not have significantly different mutation and neoantigen numbers (**Fig. S7C, D**), suggesting other molecular mechanisms

may drive anti-tumor immunity in tumors like HNSC. We also correlated Immune Class with copy number alterations of specific driver genes (**Fig. S7E**).

Active Immune Class is linked with Favorable Prognosis

We then explored the prognostic implications of immune molecular subgroups by correlating them with clinicopathological variables (**Table 1**). The Active Immune Class was associated with early pathologic T-status (P =0.01), primary site of oropharynx (P <0.001), and human papillomavirus (HPV) infection (63% vs. 13% in Exhausted by p16 status, P <0.001; 51% vs. 0% in Exhausted by ISH status, P <0.001).

Survival analysis according to immune molecular subgroups showed that, patients with Immune Class had significantly better overall survival (OS) than the non-Immune Class (P =0.03; **Fig. 2A**); we also observed a trend for better disease-free survival (DFS) (P =0.11; **Fig. 2B**). Patients with the Active Immune Class had a tendency to have better OS (P =0.07) and DFS (P =0.06) (**Fig. 2C, D**) than the Exhausted and non-Immune Classes. Compared with non-Active Immune Class, Active Immune Class was associated with significantly better OS (P =0.03) and DFS (P =0.02) (**Fig. 2E, F**). In multivariate analyses, immune molecular subgroups was retained as independent prognostic factor for OS (P =0.04), and was marginally significant for DFS (P =0.05) (**Table S7**). A relatively higher area under the curve was shown for immune molecular subgroups versus IFN signature (**Fig. S8**).

Validation of the novel immune molecular subgroups

The presence of Immune Class was further evaluated in six additional datasets (n = 838

HNSC samples) using the 115 gene-expression based immune classifier (**Table S3**). Similar to our training cohort, the percentage of patients allocated to Immune Class was ~30–40% across the datasets (range 27–43%) (**Fig. S9**). We take GSE65858, the largest dataset, as an example. 27% of HNSC samples were predicted within the Immune Class, and we confirmed the enrichment of immune-related signatures identifying immune cells (e.g., 13 T-cell signature, B-cell cluster; all, $P < 0.001$), IFN signature ($P < 0.001$) and enhanced cytolytic activity ($P < 0.001$) in the Immune Class (**Fig. S9F**). In addition, 21% of the Immune Class showed presence of the activated stroma signature, along with over-expression of stromal enrichment score, M2 macrophages and WNT/TGF-β signatures, recapitulating the Exhausted Immune Class (**Fig. S9F**). Correlation with clinical outcomes confirmed that patients within the Active Immune Class had significantly better OS ($P = 0.02$) and progression-free survival ($P = 0.03$) (**Fig. S10A, B**). In other datasets, molecular characterization also showed the enrichment of the immune-related signatures in Immune Class, and distribution features among Exhausted and Active Immune Classes. Survival analyses perform in other two datasets with available data showed that Active Immune Class shows significantly better OS and had a tendency to have better metastasis-free survival (**Fig. S10C, D**).

Finally, we tested the capacity of the immune molecular subgroups to predict response to immunotherapy. We compared the gene expression profile of our immune molecular subgroups with that of a recently published melanoma cohort [12]. Subclass mapping revealed that Immune Class, in particular the Active Immune Class, was similar to the melanoma tumors responding to PD-1 blockade ($P=0.04$ and $P=0.01$, respectively; **Fig.**

S11).

DISCUSSION

Recently early reports from trials with immunotherapy, especially checkpoint inhibitors, have shown promising results with the potential for improved disease control in advanced HNSC patients [1-4, 13]. However, their inconsistent results in exploratory biomarker analyses highlight the need to identify ideal subgroups for immunotherapy in HNSC, which remains a major challenge in the era of immuno-oncology.

The recent single-cell analysis suggests that HNSC tumors are complex mixtures of stromal cellular elements [6]. NMF is a virtual separation approach that could help separate molecular signatures of tissue compartments from measurements of bulk tumor samples. It is well suited for biological data as it constrains all sources to be positive in nature, and reflect the goal of identifying positive gene expression exemplars [7]. In this study, we use NMF to deconvolute the gene expression data of HNSC samples, and present a new characterization of the HNSC tumor immune landscape. Close to 40% of HNSCs were found to belong to the Immune Class, whose molecular characteristics, including the presence of inflammatory response, high immune cell infiltration, enhanced cytolytic activity, and active IFN signaling, highly resemble those of cancers most responsive to immunotherapy [14, 15]. Nonetheless, the presence of an immune phenotype does not absolutely predict immunotherapy response. Further dissection of the Immune Class gene expression profile allowed us to elucidate such interactions and identify the Active and Exhausted subtypes. While T cell–related immune signatures did not differ between the two subtypes, the Active Immune Class showed enrichment of B cell–related immune

signatures, cytolytic activity and proinflammatory M1 macrophages, suggesting that the humoral immune response may play an important role in influencing intratumoral immune response activation and exhaustion in HNSC. Conversely, the Exhausted Immune Class was characterized by tumor-promoting signals (e.g., activated stroma, anti-inflammatory M2 macrophages). In particular, WNT/TGF-β signaling pathway activation was significantly enriched in the Exhausted subtype; TGF-β regulates tumor–stroma interactions, EMT, angiogenesis, and metastasis, and can suppress the host immune response. The IFN signature [11] did not differ between the Active and Exhausted subtypes, suggesting that it may not fully satisfy the need to tailor immunotherapy in HNSCs.

As expected, patients with the Active Immune Class had a significantly favorable prognosis. Integration of immune molecular subgroups with the four known HNSC molecular subtypes, which were classified mainly based on genome-wide profiling [16, 17], revealed that the Active subtype was more common in the less aggressive atypical subtype. This may partially explain the different features between the four molecular subtypes. Recently, the Pan-Cancer Atlas of TCGA identified six pan-cancer immune subtypes [18]. When we integrated these immune subtypes in this study, we observed most of HNSCs belong to the wound healing (25%) or IFN-γ dominant (74%) subtypes, while other four subtypes only account for 1% of HNSCs. Thus, it seems that the pan-cancer immune subtypes may not be fully applicable to HNSC.

Interestingly, neither mutational burden nor neoantigen load was associated with the immune molecular subgroups. We previously also observed no correlation between PD-L1, CD8A, or cytolytic activity expression and mutation or neoantigen number in HNSC

and other tumors (e.g. glioblastoma, prostate cancer) [19]. Similar lack of such correlation has been described in pancreatic cancer and hepatocellular carcinoma as well [8, 20, 21]. These results suggest that, unlike melanoma or lung cancer, other molecular mechanisms may drive anti-tumor immunity in tumors like HNSC. In these settings, neoantigen quality or clonality, rather than quantity, may influence the immune reactivity [22]. We also observed that Immune Class was associated with lower copy number alteration burden of driver genes (e.g., *PIK3CA*, *NSD1*, *NOTCH1*). This indicates that tumor aneuploidy in specific oncogenic pathways may play a role in regulating the immune response in HNSC [23]. Other mutation-independent mechanisms, such as HPV infection, might also affect the immune infiltrate. We found significantly more HPV-positive tumors in the Active Immune Class. Trials evaluating nivolumab or pembrolizumab in advanced HNSC have also reported relatively higher response rates in HPV-positive patients [1-3]. That HPV-positive tumors have a higher degree of tumor inflammation may explain this [24]. These results suggest that the immune response in HNSC is more likely to be regulated by a combination of tumor-intrinsic factors, based on the tumor genetic make-up (e.g. aneuploidy, activation of specific signaling, immune-related molecule expression), and tumor-extrinsic factors present in the tumor microenvironment (e.g., TIL, HPV infection).

Successful replication in six independent datasets supported the robustness of the immune molecular subgroups. When tested in a melanoma cohort, our HNSC Immune Class, particularly the Active Immune Class was associated with the melanoma tumors responding to PD-1 blockade, confirming its predictive value. Nevertheless, it should be noted that our findings require further validation in immunotherapy-treated HNSC tumors

(both locoregional and advanced). Our findings should be interpreted with this limitation in mind.

Understanding the landscape of tumor-immune microenvironment is critical for improving the efficacy of current immunotherapies. For example, patients with the Active Immune Class may benefit from single-agent immune checkpoint blockades, while patients with the Exhausted Immune Class may benefit from TGF-β inhibition plus immune checkpoint blockade. In this regard, a phase 1b/2 clinical trial testing the novel TGF-β inhibitor galunisertib in combination with nivolumab in advanced solid tumors is ongoing (NCT02423343). For the remaining patients who lack detectable immune reactions, combination therapy designed to attract T cell infiltration into the tumor microenvironment and avoid their being turned off, e.g., combined anti–CTLA-4 and anti–PD-1/PD-L1 therapy, might be prioritized [25, 26]. Inducing a type I IFN response would also be an approach [15]. Further dissection of the oncogenic mechanisms responsible for immune exhaustion or ignorance could aid in modifying the tumor immune profile and yield additional combination strategies.

In summary, we introduce novel immune molecular subgroups in HNSC. Classification of HNSC into these novel subgroups might aid the identification of ideal candidates and tailor optimal immunotherapeutic strategies. These findings warrant further investigations in larger HNSC cohorts receiving immune checkpoint therapies.

Acknowledgements

We thank Dr. Robert L. Ferris (Cancer Immunology Program, UPMC Hillman Cancer Center, Pittsburgh, PA, USA) for his helpful comments on this study. We thank the staff

members of the Cancer Genome Atlas for their involvement in the cBioPortal for Cancer Genomics Program.

Funding

This work was supported by grants from the Natural Science Foundation of Guang Dong Province (No. 2017A030312003), National Natural Science Foundation of China (No. 81802707), Health & Medical Collaborative Innovation Project of Guangzhou City, China (201803040003), Innovation Team Development Plan of the Ministry of Education (No. IRT_17R110), and the Overseas Expertise Introduction Project for Discipline Innovation (111 Project, B14035)

Conflict of interest statement

We declare that we have no conflicts of interest.

References

1. Ferris RL, Blumenschein G, Jr., Fayette J et al. Nivolumab for Recurrent Squamous-Cell Carcinoma of the Head and Neck. N Engl J Med 2016; 375: 1856-1867.

2. Seiwert TY, Burtness B, Mehra R et al. Safety and clinical activity of pembrolizumab for treatment of recurrent or metastatic squamous cell carcinoma of the head and neck (KEYNOTE-012): an open-label, multicentre, phase 1b trial. Lancet Oncol 2016; 17: 956-965.

3. Chow LQM, Haddad R, Gupta S et al. Antitumor Activity of Pembrolizumab in

Biomarker-Unselected Patients With Recurrent and/or Metastatic Head and Neck Squamous Cell Carcinoma: Results From the Phase Ib KEYNOTE-012 Expansion Cohort. J Clin Oncol 2016; 34: 3838-3845.

4. Bauml J, Seiwert TY, Pfister DG et al. Pembrolizumab for Platinum- and Cetuximab-Refractory Head and Neck Cancer: Results From a Single-Arm, Phase II Study. J Clin Oncol 2017; 35: 1542-1549.

5. Zou W, Wolchok JD, Chen L. PD-L1 (B7-H1) and PD-1 pathway blockade for cancer therapy: Mechanisms, response biomarkers, and combinations. Sci Transl Med 2016; 8: 328rv324.

6. Puram SV, Tirosh I, Parikh AS et al. Single-Cell Transcriptomic Analysis of Primary and Metastatic Tumor Ecosystems in Head and Neck Cancer. Cell 2017; 171: 1611-1624 e1624.

7. Moffitt RA, Marayati R, Flate EL et al. Virtual microdissection identifies distinct tumor- and stroma-specific subtypes of pancreatic ductal adenocarcinoma. Nat Genet 2015; 47: 1168-1178.

8. Sia D, Jiao Y, Martinez-Quetglas I et al. Identification of an Immune-specific Class of Hepatocellular Carcinoma, Based on Molecular Features. Gastroenterology 2017; 153: 812-826.

9. Brunet JP, Tamayo P, Golub TR, Mesirov JP. Metagenes and molecular pattern discovery using matrix factorization. Proc Natl Acad Sci U S A 2004; 101: 4164-4169.

10. Yoshihara K, Shahmoradgoli M, Martinez E et al. Inferring tumour purity and stromal and immune cell admixture from expression data. Nat Commun 2013; 4: 2612.

11. Chow LQM, Mehra R, Haddad RI et al. Biomarkers and response to pembrolizumab (pembro) in recurrent/metastatic head and neck squamous cell carcinoma (R/M HNSCC). Journal Of Clinical Oncology 2016; 34.

12. Chen PL, Roh W, Reuben A et al. Analysis of Immune Signatures in Longitudinal Tumor Samples Yields Insight into Biomarkers of Response and Mechanisms of Resistance to Immune Checkpoint Blockade. Cancer Discov 2016; 6: 827-837.

13. Ferris RL, Saba NF, Gitlitz BJ et al. Effect of Adding Motolimod to Standard Combination Chemotherapy and Cetuximab Treatment of Patients With Squamous Cell Carcinoma of the Head and Neck: The Active8 Randomized Clinical Trial. JAMA Oncol 2018.

14. Rooney MS, Shukla SA, Wu CJ et al. Molecular and genetic properties of tumors associated with local immune cytolytic activity. Cell 2015; 160: 48-61.

15. Bald T, Landsberg J, Lopez-Ramos D et al. Immune cell-poor melanomas benefit from PD-1 blockade after targeted type I IFN activation. Cancer Discov 2014; 4: 674-687.

16. Chung CH, Parker JS, Karaca G et al. Molecular classification of head and neck squamous cell carcinomas using patterns of gene expression. Cancer Cell 2004; 5: 489-500.

17. Cancer Genome Atlas N. Comprehensive genomic characterization of head and neck squamous cell carcinomas. Nature 2015; 517: 576-582.

18. Thorsson V, Gibbs DL, Brown SD et al. The Immune Landscape of Cancer. Immunity 2018.

19. Chen YP, Zhang Y, Lv JW et al. Genomic Analysis of Tumor Microenvironment

Immune Types across 14 Solid Cancer Types: Immunotherapeutic Implications. Theranostics 2017; 7: 3585-3594.

20. Balli D, Rech AJ, Stanger BZ, Vonderheide RH. Immune Cytolytic Activity Stratifies Molecular Subsets of Human Pancreatic Cancer. Clin Cancer Res 2017; 23: 3129-3138.

21. Colli LM, Machiela MJ, Myers TA et al. Burden of Nonsynonymous Mutations among TCGA Cancers and Candidate Immune Checkpoint Inhibitor Responses. Cancer Res 2016; 76: 3767-3772.

22. McGranahan N, Furness AJ, Rosenthal R et al. Clonal neoantigens elicit T cell immunoreactivity and sensitivity to immune checkpoint blockade. Science 2016; 351: 1463-1469.

23. Davoli T, Uno H, Wooten EC, Elledge SJ. Tumor aneuploidy correlates with markers of immune evasion and with reduced response to immunotherapy. Science 2017; 355.

24. Lyford-Pike S, Peng S, Young GD et al. Evidence for a role of the PD-1:PD-L1 pathway in immune resistance of HPV-associated head and neck squamous cell carcinoma. Cancer Res 2013; 73: 1733-1741.

25. Wolchok JD, Kluger H, Callahan MK et al. Nivolumab plus ipilimumab in advanced melanoma. N Engl J Med 2013; 369: 122-133.

26. Huang RR, Jalil J, Economou JS et al. CTLA4 blockade induces frequent tumor infiltration by activated lymphocytes regardless of clinical responses in humans. Clin Cancer Res 2011; 17: 4101-4109.

Figure legends

Fig. 1. Identification of head and neck squamous cell carcinoma (HNSC) immune molecular subgroups. (A) Consensus-clustered heat map of HNSC samples (TCGA dataset, n = 522) using exemplar genes of the non-negative matrix factorization (NMF) immune factor and refined by Random Forest; 211/522 (40%) samples were classified into Immune Class. **(B)** Nearest Template Prediction (NTP) using a signature capturing activated stroma identified two distinct immune response subtypes: Exhausted (56/211, 27%; purple bar) and Active (155/211, 73%; blue bar). In the heat map, high and low single-sample gene set enrichment scores are represented in red and blue, respectively. Positive prediction of activated stroma signature as per NTP is indicated in red and its absence is in grey. IFN, interferon; TLS, tertiary lymphoid structure.

Fig. 2. Kaplan–Meier survival analysis according to immune molecular subgroups. Kaplan–Meier plots of overall survival **(A, C, E)** and disease-free survival **(B, D, F)** according to Immune and non-Immune Classes **(A and B)**, Active Immune, Exhausted Immune, and non-Immune Classes **(C and D)**, and the Active Immune and non-Active Immune Classes **(E and F)**. *P*-values were calculated by log-rank test.

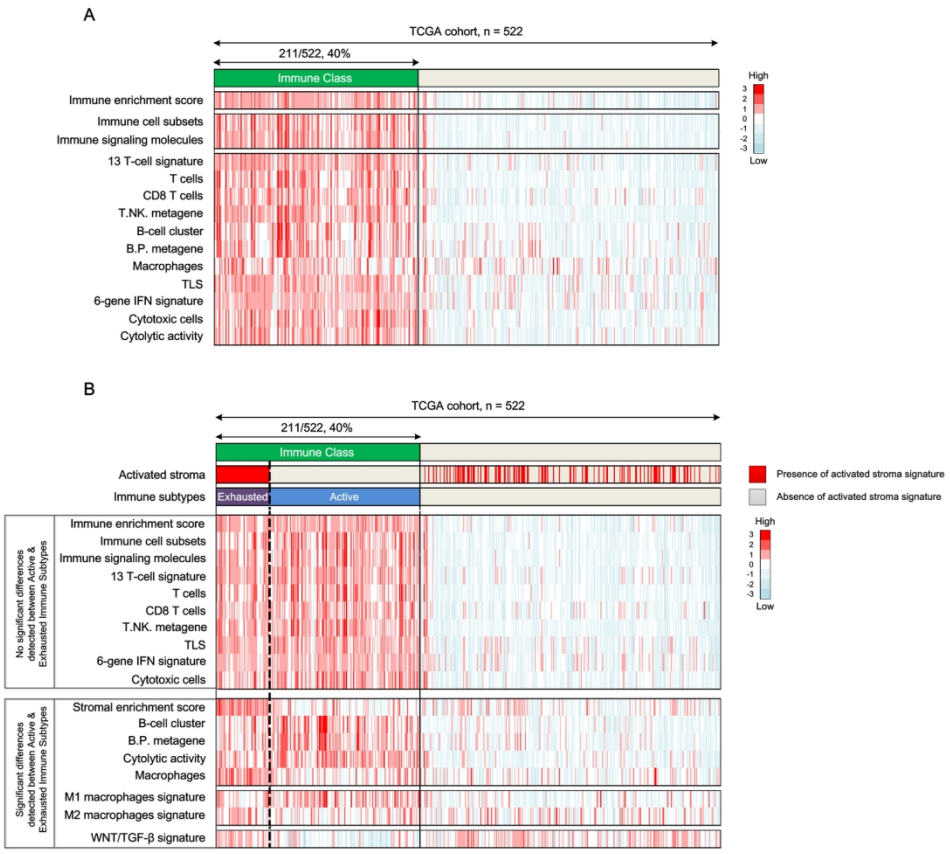

Fig. 1. Identification of head and neck squamous cell carcinoma (HNSC) immune molecular subgroups. (A) Consensus-clustered heat map of HNSC samples (TCGA dataset, n = 522) using exemplar genes of the non-negative matrix factorization (NMF) immune factor and refined by Random Forest; 211/522 (40%) samples were classified into Immune Class. (B) Nearest Template Prediction (NTP) using a signature capturing activated stroma identified two distinct immune response subtypes: Exhausted (56/211, 27%; purple bar) and Active (155/211, 73%; blue bar). In the heat map, high and low single-sample gene set enrichment scores are represented in red and blue, respectively. Positive prediction of activated stroma signature as per NTP is indicated in red and its absence is in grey. IFN, interferon; TLS, tertiary lymphoid structure.

155x140mm (300 x 300 DPI)

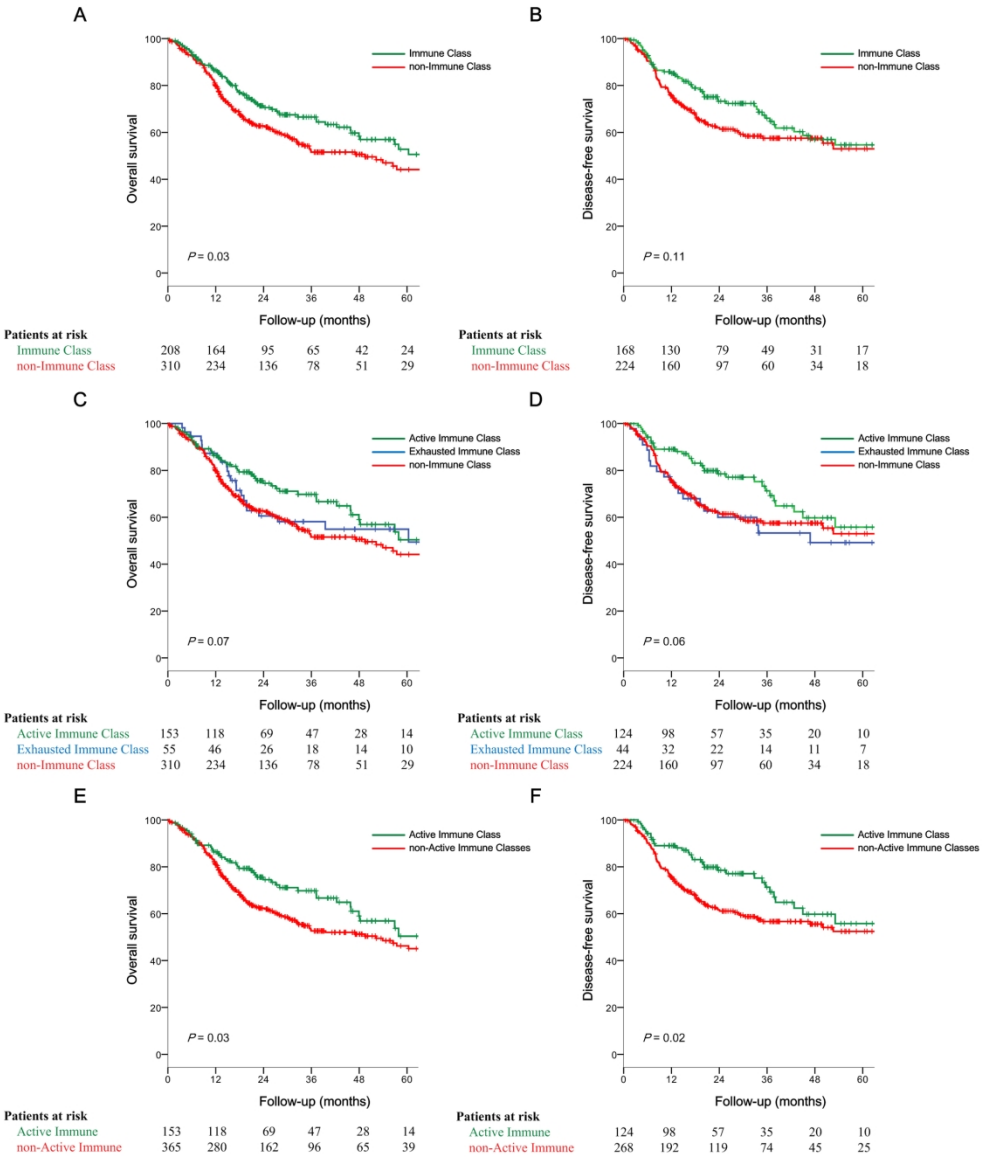

Fig. 2. Kaplan–Meier survival analysis according to immune molecular subgroups. Kaplan–Meier plots of overall survival (A, C, E) and disease-free survival (B, D, F) according to Immune and non-Immune Classes (A and B), Active Immune, Exhausted Immune, and non-Immune Classes (C and D), and the Active Immune and non-Active Immune Classes (E and F). P-values were calculated by log-rank test.

184x213mm (300 x 300 DPI)

Table 1. Correlation between microenviroment-based immune molecular subgroups and clinicopathological variables in TCGA set

Variable*	Exhausted Immune Class (n = 56)	Active Immune Class (n = 155)	non-Immune Class (n = 311)	*P* value
Median age (IQR)	65 (58-73)	60 (55-69)	60 (52-67)	0.02
Gender, male	41 (75%)	109 (70%)	234 (75%)	0.52
Primary site				< 0.001
Oral Cavity	36 (65%)	76 (49%)	203 (65%)	
Oropharynx	6 (11%)	44 (28%)	31 (10%)	
Larynx & Hypopharynx	13 (24%)	35 (23%)	77 (25%)	
Smoking				
Non-smoker	8 (15%)	43 (28%)	66 (22%)	0.09
Former & current smoker	46 (85%)	108 (72%)	237 (78%)	
Alcohol history				0.98
No	18 (33%)	48 (31%)	96 (32%)	
Yes	37 (67%)	105 (69%)	206 (68%)	
Pathologic T				0.01
T1-2	17 (35%)	67 (52%)	101 (36%)	
T3-4	32 (65%)	61 (48%)	181 (64%)	
Pathologic N				0.66
N0-1	25 (52%)	67 (60%)	151 (58%)	
N2-3	23 (48%)	45 (40%)	110 (42%)	
Pathologic Tumor Stage				0.25
Stage I-II	13 (27%)	31 (26%)	54 (19%)	
Stage III-IV	36 (73%)	88 (74%)	224 (81%)	

HPV status P16 IHC				< 0.001
Negative	14 (88%)	15 (37%)	43 (80%)	
Positive	2 (13%)	26 (63%)	11 (20%)	
HPV status ISH				< 0.001
Negative	13 (100%)	17 (49%)	35 (92%)	
Positive	0 (0%)	18 (51%)	3 (8%)	
Events				
Progression	20 (45%)	35 (28%)	89 (40%)	0.04
Death	25 (45%)	52 (34%)	145 (47%)	0.02

Abbreviations: HPV, human papillomavirus; IHC, immunohistochemistry; ISH, in-situ hybridization.

*Variables included in this table had < 20% of available values except for HPV P16 IHC, HPV status ISH, and disease progression.